ELSEVIER

Coordination Chemistry Reviews
211 (2001) 295–315

COORDINATION CHEMISTRY REVIEWS

www.elsevier.com/locate/ccr

Excited state processes at sensitized nanocrystalline thin film semiconductor interfaces

Craig A. Kelly, Gerald J. Meyer *

Department of Chemistry, Johns Hopkins University, Baltimore, MD 21211, USA

Received 14 September 1999; accepted 10 January 2000

Dedicated to Professor Arthur W. Adamson on the occasion of his 80th birthday

Contents

Abstract 295
1. Introduction 296
2. Literature results 298
2.1. Charge injection and excited-state decay 298
2.1.1. The rate of electron injection inferred from dynamic quenching of the excited state 299
2.1.2. Measurements of the electron injection rate constant 301
2.1.3. Ultra-fast transient absorbance measurements 306
2.1.4. Excited state processes 308
3. Conclusions 312
Acknowledgements 313
References 313

Abstract

The existing and potential technological importance of nanocrystalline semiconductor thin films sensitized to visible light by molecular chromophores have initiated considerable efforts toward understanding the detailed mechanisms of photoprocesses occurring at the interface. However, such studies are made difficult by the complex nature of kinetic processes observed following light excitation. In this paper, we review literature reports of excited-state processes in these materials and attempt to clarify the underlying mechanisms responsible for the complex kinetic behavior typically observed. © 2001 Elsevier Science B.V. All rights reserved.

Keywords: Excited state processes; Nanocrystalline; Thin film semiconductor interfaces

* Corresponding author. Tel.: +1-410-5167319; fax: +1-410-5168420.

PII: S0010-8545(00)00285-X

1. Introduction

In pioneering studies almost 30 years ago, Adamson and co-workers demonstrated that the excited state of tris(2,2′-bipyridine)ruthenium(II), $Ru(bpy)_3^{2+}$, could promote bimolecular electron transfer reactions in fluid solution [1]. This work has paved the way toward the use of this, and related coordination compounds, for the photoinitiation of interfacial electron transfer as a means to convert light into an electrical response. This optical–electronic interface is an area of tremendous interest for applications ranging from solar cells, optical switches and optical sensing to signal transduction applications [2–4]. Wide band gap semiconductors such as TiO_2, SnO_2, WO_3, and $SrTiO_3$, are ideal materials for optoelectronic applications because of their low cost and photochemical stability [5,6]. However, wide band gap materials suffer from spectral sensitivity limited to UV, a spectral region unsuitable for many applications. This difficulty has been overcome by sensitizing the semiconductors to longer wavelengths of light through surface modification with molecular chromophoric compounds [7]. Tremendous progress has been made by photoelectrochemists developing physical models of the interfacial charge-transfer processes [8–13]. A critical problem with early investigations, in which single-crystal semiconductors were sensitized, was the very low light harvesting efficiency [14] of a monolayer on a planar surface due to the limited optical path length [15]. The inability to absorb a significant portion of incident photons greatly diminishes the efficiency of the electrical response.

To increase the light harvesting efficiency, Grätzel and co-workers prepared high surface area mesoporous nanocrystalline, TiO_2 (anatase), thin films (ca. 10 m thick) on conductive glass substrates [16–20]. The enormous surface area of the films allow high light harvesting efficiency even at monolayer surface coverages. Surface areas accessible by the chromophore were measured to be around 1000 times that of a flat surface [20]. Surface coverages of 1.3×10^{-7} mol cm^{-2} were achieved allowing absorption of $> 99\%$ of the photons transmitted though the cell windows in the ca. 450–550 nm wavelength range after correcting for scatter. Importantly, the high transparency of the naked TiO_2 films at wavelengths longer than ca. 360 nm, Fig. 1 [21], allows for the direct study of light to electrical energy conversion using time resolved spectroscopic methods previously limited to colloidal suspensions [22]. Furthermore, the Fermi level within each semiconductor particle can be controlled potentiostatically [23–36]. Thus, both the spectroscopic and electrochemical properties of the material can be probed. Reviews of this area have appeared [4,22,37–40].

The focus of the present review will be on the excited-state chemistry of Ru(II) polypyridyl complexes bound to semiconductor thin films, including natural (i.e. radiative and nonradiative) decay, surface mediated reactions, and electron injection into the semiconductor. The polypyridine ligand abbreviations used throughout the text are given in Fig. 2. Fig. 3 shows the key, single molecule, reactions that will be discussed. Following the absorption of a photon by the resting oxidation state of the surface attached photosensitizer, P^0, the resulting excited state, P^{0*}, may inject an electron into the semiconductor support, characterized by a rate constant,

k_{inj}. The nature of the acceptor state in the semiconductor is uncertain and may be represented by the conduction band or a trap site, for example see Ref. [41]. In the absence of a viable electron donor, the hole resides on the surface as an oxidized sensitizer, P^+. In competition with electron injection is deactivation of the excited state to the ground state by radiative, k_r, and nonradiative, k_{nr}, decay.

Investigations of nanocrystalline thin films related to charge recombination between the injected electron and the oxidized dye molecule [42], electron transport through the interconnected nanocrystalline thin film network [43–51], and lateral hole transport via electron hopping between adjacent compounds [36,52], will not be reviewed here. Spectroscopic studies of semiconductor colloids, in which direct ultraviolet excitation of the solid was used to quantify electron/hole recombination, trapping and interfacial electron transfer processes have been previously reviewed and will not be discussed further here [53–56]. Heimer and Meyer have previously reviewed the luminescence properties of sensitizers bound to colloidal suspensions and colloidal films [57]. Investigations of sensitizing TiO_2 colloidal solutions to visible light with molecular sensitizers have been reviewed [58,59], but attention is called to the work of Fox [60–62], Ford and Rodgers [63–68], Grätzel [69,70] and Kamat [71–74].

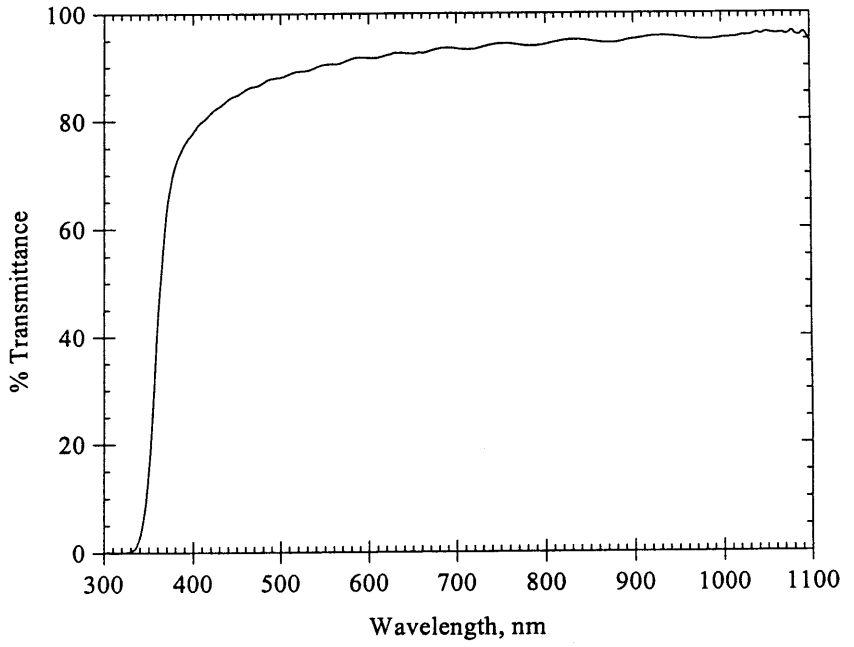

Fig. 1. Typical transmission spectrum of a nanocrystalline TiO_2 (anatase) thin film, ca. 10 microns thick, on a glass slide immersed diagonally in a 10 mm quartz cuvette in neat acetonitrile [21]. The spectrum is corrected for absorption and scatter from the cuvette, acetonitrile and glass slide.

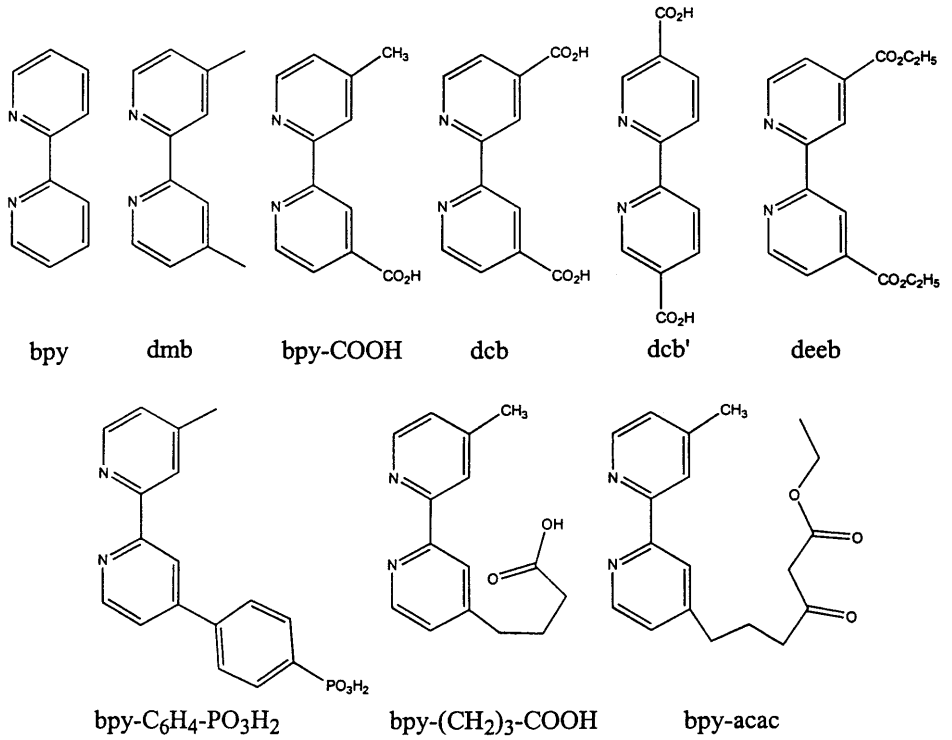

Fig. 2. Bipyridine ligands and abbreviations used in the text.

2. Literature results

2.1. Charge injection and excited-state decay

Electron injection into a semiconductor support, S, initiated by photoexcitation of a surface bound photosensitizer, P^0, Eq. (1), may proceed by two different routes.

$$P^0/S + h\nu \rightarrow P^{0*}/S \quad (1)$$

The first involves direct oxidation of the excited state by the semiconductor and is often referred to as oxidative quenching, Eq. (2) [75].

$$P^{0*}/S \rightarrow P^{\bullet +}/S(e^-) \quad (2)$$

Alternatively reduction of the excited state with an electron donor by a bimolecular pathway, D (Eq. (3)), or unimolecularly by a covalently attached donor in a supramolecular complex in the photosensitizer, $D–P^0$ (Eq. (4)), may be possible [76]. The resulting reduced photosentsitizer, $P^{\bullet -}$, may inject an electron into the semiconductor, Eqs. (5) and (6).

$$P^0*/S + D \rightarrow P^{\bullet -}/S + D^{\bullet +} \quad (3)$$

$$D\text{–}P^0*/S \rightarrow D^{\bullet +}\text{–}P^{\bullet -}/S \quad (4)$$

$$P^{\bullet -}/S \rightarrow P^0*/S(e^-) \quad (5)$$

$$D^{\bullet +}\text{–}P^{\bullet -}/S \rightarrow D^{\bullet +}\text{–}P^0/S(e^-) \quad (6)$$

The latter example, often referred to as reductive quenching [75], has been inferred from the photoelectrochemical investigations [77], and has recently been directly observed by Thompson et al. using transient absorption with phenothiazine as the electron donor [78]

The oxidative quenching pathway is the more commonly considered route for electron injection. However, the reductive quenching pathway may be a useful alternative mechanism to sensitize wide band gap semiconductors using sensitizers that possess excited-state reduction potentials insufficient for electron injection.

2.1.1. The rate of electron injection inferred from dynamic quenching of the excited state

Time resolved investigations of the electron injection rate by reductive quenching pathway, Eq. (5), has been limited to the work of Thompson et al., where only an upper limit, $k_{inj} > 1.2 \times 10^{-8}$ was reported [78]. Many attempts have been made to measure the rate of electron injection by the oxidative mechanism, Eq. (2), in nanocrystalline thin films. One approach is based on the assumption that the rate of photoluminescence, PL, decay of a photosensitizer bound to a semiconductor is

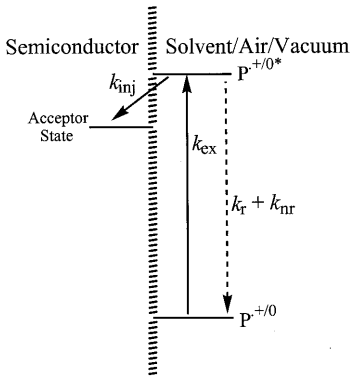

Fig. 3. Photophysical and photochemical processes referred to in the text. The hashed line represents the semiconductor interface with a solvent, air or vacuum. $P^{\bullet +/0}$ is the oxidized/resting oxidation state of the surface bound photosensitizer, $P^{\bullet +/0*}$ is the oxidized/excited state of the photosensitizer. The 'acceptor state' is a hypothetical semiconductor state in which the injected electron resides. This state may encompass the state into which the electron is injected and/or the state from which the electron recombines with the oxidized photosensitizer. The kinetic processes are defined by: k_{ex}, the rate constant for optical excitation of the photosensitizer, k_r and k_{nr}, the radiative and nonradiative decay rate constants of the excited state of the photosensitizer, and k_{inj}, the rate constant for electron injection from the excited state of the photosensitizer into the semiconductor.

the sum of radiative and nonradiative excited state deactivation, Eq. (7), and interfacial charge transfer, Eq. (2).

$$P^0*/S \xrightarrow{k_r + k_{nr}} P^0/S + (h\nu \text{ or } \Delta) \quad (7)$$

The rate constant for interfacial charge transfer may then be obtained by subtracting the natural lifetime, i.e. the sum of the radiative, k_r, and nonradiative, k_{nr}, decay rate constants, from the observed decay rate constant, k_{obs}, Eq. (8).

$$k_{inj} = k_{obs} - (k_r + k_{nr}) \quad (8)$$

The natural lifetime may be obtained, for example, from the decay of the excited state on an insulator, i.e. where electron injection is not thermodynamically possible, but where the sensitizer environment is similar to that on a semiconductor. Investigations of this type have been driven by observations that the excited-state lifetime is longer on insulators than on semiconductors where electron injection is possible.

One difficulty encountered in applying this approach has been the common observation of nonexponential kinetics for the excited-state decay on either semiconductor or insulator surfaces. It is generally believed that the nonexponential kinetics of excited-state decay in heterogeneous environments is the result of an underlying distribution of first-order processes. The apparent distribution of first-order rate constants has been attributed to varying surface binding modes or local environment of the sensitizer, e.g. different crystal faces, grain boundaries, surface morphology, surface defects, etc., on the semiconductor surface. This argument has gained support from the single molecule luminescence measurements of Lu and Xie [79]. These authors observed that, while single molecules of cresyl violet on the surface of indium tin oxide, ITO, decay with exponential kinetics, a distribution of first-order decay rate constants, covering the range from ~ 100 to 700 ps, was observed for a sample of 40 molecules. The excited-state decay of the molecules probed was attributed to electron injection into ITO but a fraction of the excited states were reported to have decayed without electron injection, with lifetimes > 2 ns.

The observation of nonexponential processes drastically hinders quantitative analysis of the kinetics, and therefore mechanistic interpretations, of the excited-state processes on the semiconductor supports. To address this issue, a variety of approaches have been adopted in an attempt to extract kinetic information that is useful for material characterization of the interfacial chemical reactions. One approach has been to use a multiexponential model, normally based on the sum of two to four exponentials, to represent the presumed underlying distribution of rate constants [80]. A disadvantage of this model is that parameter correlation of the variables, (the number of variables for a multiexponential fit is $2i$ where i is the number of first-order components) can become significant. The alternative is to assume a continuous distribution of first-order rate constants. Skewed distributions, such as the Levy or log-normal, have been shown to fit excited state kinetics on semiconduct or surfaces adequately [81]. One advantage of such models, over fits based on a sum of several exponential processes, is that only three variables are

required for the fit, i.e. characteristic rate constant, rate constant distribution width, and initial amplitude. However, such functions can result in distribution widths covering several orders of magnitude in rate constants [81]. While a distribution of rate constants is anticipated [79], factors $> 10^4$ s^{-1} seem physically unrealistic. The kinetics of excited-state decay on the semiconductor surfaces will be returned to below.

2.1.2. Measurements of the electron injection rate constant

Eichberger and Willig reported the first attempt to time resolve electron injection from the excited state of a ruthenium(II) polypyridine complex on a nanocrystalline thin film [82]. These authors followed the luminescent decay of $Ru(dcb)_2(OH_2)_2^{2+}$ on nanocrystalline TiO_2 thin films (presumably in ultra-high vacuum) as a function of surface coverage, following excitation between 580 and 605 nm with a 5 ps laser pulse. The emission lifetime was found to be dramatically shortened on the semiconductor surface compared to the solution lifetime. The stationary state photoelectrochemical current efficiency was found to be near unity, implying near unit quantum yields for electron injection. In cases of both low and high surface loading of the sensitizer, the emission signal was convoluted with the laser pulse width yielding an upper lifetime limit of $\tau < 7$ ps, presumably corresponding to a electron injection time constant.

The first transient adsorption measurements of dye sensitized, nanocrystaline thin films, were carried out by O'Regan and co-workers [34]. These authors followed the absorbance change at 480 nm following a 530 nm, ca. 10 ns pulse width, excitation of $Ru(dcb)_3^{2+}$ on nanocrystalline TiO_2 films immersed in aqueous 0.2 M $LiClO_4$ at pH 3. The film was externally biased over the range -0.8–0.6 V versus SCE. At negative applied bias, the excited state was found to luminesce strongly and current generation was near zero. Positively biasing the electrode resulted in quenching of the luminescence and optimized photocurrent generation. Transient absorption measurements over the potential range examined, demonstrated rapid loss of the Ru(II) precursor that could not be time resolved from the laser pulse. The rapid formation of the transient signal was attributed to electron injection, $k_{inj} > 10^8$ s^{-1} [34]. However, at the wavelength probed it was not possible to distinguish if loss of the Ru(II) precursor is the result of excited state or oxidized sensitizer formation [83]. The strong photoluminescent signal observed at negative bias clearly indicates the presence of long-lived excited states under those conditions [34]. The observed transient absorption signal therefore possesses both excited state and oxidized sensitizer contributions in a ratio that is dependent on the applied bias. At -0.45 V versus SCE, the recovery of the ground state proceeds with a rate constant of 1.5×10^6 s^{-1}, similar to that for excited-state decay of the complex in solution [84].

Willig and co-workers studied the luminescent decay of the trinuclear compound $Ru(dcb)_2(\mu\text{-}(CN)Ru(CN)(bpy)_2)_2^{2+}$, Fig. 4 [85]. In ethanol solution, the excited state exhibits a lifetime of 93 ns. Surprisingly, the lifetime is reduced to 3 ns at high solution concentrations, i.e. $> 10^{-5}$ M. This was attributed to aggregation. On nanocrystalline TiO_2 the emission decayed by nonexponential kinetics with the

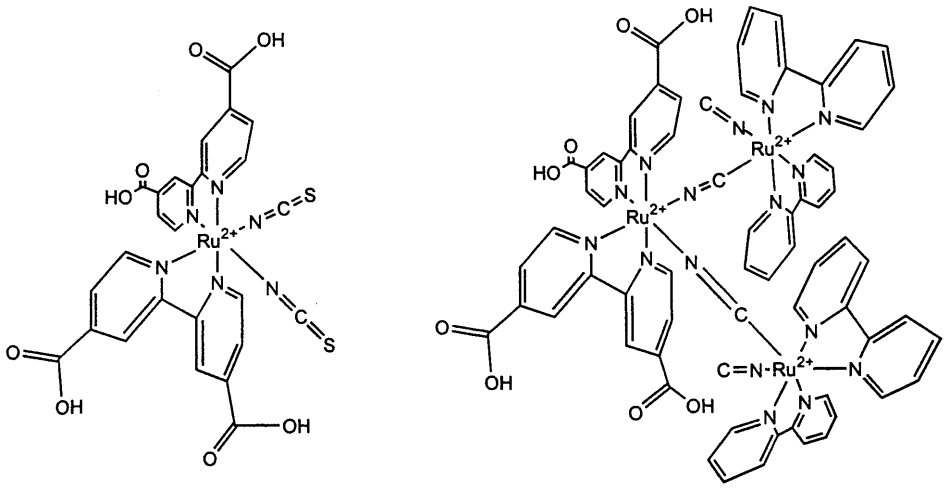

Fig. 4. Structures of *cis*-$Ru(dcb)_2(NCS)_2$ and $Ru(dcb)_2(\mu\text{-}(CN)Ru(CN)(bpy)_2)_2^{2+}$.

major component (90%), decaying with a rate constant of $5.8 \times 10^9\ s^{-1}$. The slow component was attributed to color center emission from the TiO_2. The nature of the observed color centers in TiO_2 are not clear. Ligand dissociation was noted by changes in the ground state absorption spectrum.

Bedja, Hotchandani and Kamat first reported the electron injection rate constant for $Ru(dcb)(bpy)_2^{2+}$ on nanocrystalline thin films of SnO_2 based on the emission decay kinetics of the excited state of the sensitizer [86]. The luminescence decay of $Ru(dcb)(bpy)_2^{2+}$ on alumina was reported to decay by exponential kinetics with a lifetime, $\tau = 0.26$ μs. In contrast, when the Ru(II) complex was absorbed on the thin SnO_2 films, the emission decay observed at 640 nm following a 532 nm, ca. 10 ns, laser pulse deviated from exponential kinetics. The decay was fit to a biexponential with lifetimes of 12.5 and 83.3 ns. Subtracting the rate of decay on alumina yielded the electron injection rate constants, $k_{inj} = 7.6 \times 10^7$ and $8.2 \times 10^6\ s^{-1}$ for the two components (Eq. (8)).

Heimer and Meyer have used a distributional approach to estimate the electron injection rate constant into nanocrystalline TiO_2 thin films sensitized by *cis*-$Ru(dcb)_2(CN)_2$, and other Ru(II) sensitizers [87]. The luminescence decay of *cis*-$Ru(dcb)_2(CN)_2$ on TiO_2 and ZrO_2 following 532 nm, ca. 5 ns, excitation, was monitored at 700 nm. The excited-state lifetime was found to be much longer on the insulator ZrO_2, were electron injection is not energetically favored, Fig. 5. The observed nonexponential kinetic decays were fit to a log-normal distribution of first-order rate constants (Gaussian with respect to the natural logarithm of the rate constant), to yield average lifetimes of 106 ns on ZrO_2 and 0.37 ns on TiO_2, and a

Levy distribution of first-order rate constants. Both distribution functions analytically described the data and allowed the normalized transients to be fit to two uncorrelated parameters. However, the Levy distribution of relaxation rates on TiO_2 were highly skewed and judged to be physically unreasonable and were not analyzed further, Fig. 6(a). The difference of the log-normal distributions, Eq. (8) and Fig. 6(b), yield an average value of $k_{inj} = 2.7 \times 10^9\ s^{-1}$.

Argazzi et al. studied the photoluminescence decay of $Ru(dcb)_2(CN)_2$ on nanocrystalline thin films of TiO_2 immersed in I^-/I_3^- propylene carbonate electrolyte [88]. Excitation was carried out at 460 nm, with a pulse duration of ~ 200 ps. The nonexponential emission decays on TiO_2, and on the insulator SiO_2, were fit to a Levy distribution of rate constants to yield lifetimes of < 20 and 259 ns, respectively. Analysis of the excited-state decay on TiO_2 was complicated by a ca. 80% decay within 20 ns and the possibility of the remaining 20% being due to noninjecting excited states. The difference in rate constants yields $k_{inj} > 5 \times 10^7\ s^{-1}$.

In an attempt to verify that the short excited-state lifetime of $Ru(dcb)(bpy)_2^{2+}$ measured on semiconductors was due to electron injection, Fessenden and Kamat carried out parallel microwave absorption and luminescence quenching experiments [89]. The transient microwave absorption measurements probe the enhanced absorption of the semiconductor in the microwave region after pulsed 532 nm light excitation of the sensitized material. The apparatus used had an instrument response time of 4 ns. The absorption signals are expected to be a direct measurement of the concentration of electrons in the semiconductor. The study used thin films of SnO_2, ZnO, and TiO_2 sensitized to visible light with $Ru(dcb)(bpy)_2^{2+}$. The

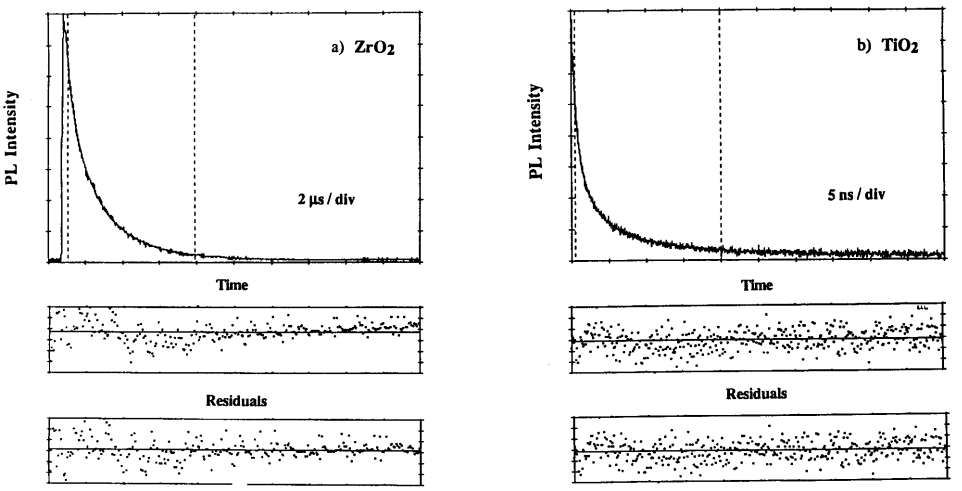

Fig. 5. Photoluminescence decays of *cis*-$Ru(dcb)_2(CN)_2$ anchored to (a) ZrO_2 and (b) TiO_2 in regenerative photoelectrochemical cells containing 0.5 M NaI/0.05 M I_2 in propylene carbonate monitored at 700 nm. A distribution analysis of these decays over the time window indicated by the dashed vertical lines was performed. Residuals based on log-normal (upper residuals) and Levy (lower residuals) distributions of first-order rate constants are shown to judge the quality of the fits.

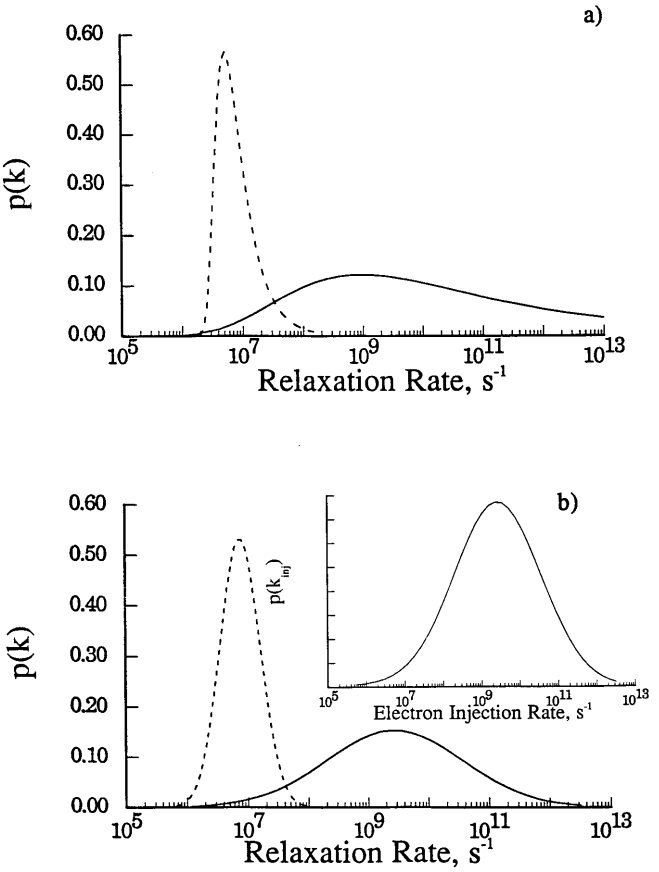

Fig. 6. Distribution of relaxation rates for the PL decays shown in Fig. 5 on (- - -) ZrO_2 or (—) TiO_2. Panel (a) depicts the Levy distribution of relaxation rates. Panel (b) shows the log-normal distribution of relaxation rates and an inset showing the distribution of electron injection rates calculated with Eq. (8).

first-order growth of the microwave signal, k_{M1}, and the fast decay component of a biexponential fit of the luminescence decay, k_{L1}, were nearly identical for films of $Ru(dcb)(bpy)_2^{2+}$ on SnO_2 ($k_{M1} = 3.0 \times 10^8$ and $k_{L1} = 2.7 \times 10^8$ s^{-1}) and ZnO ($k_{M1} = 1.0 \times 10^8$ and $k_{L1} = 1.2 \times 10^8$ s^{-1}). For films of $Ru(dcb)(bpy)_2^{2+}$ on TiO_2 the microwave signal was too weak to fit, but was reported to be similar to that for the $Ru(dcb)(bpy)_2^{2+}$/ZnO sample with $k_{L1} = 2.0 \times 10^8$ s^{-1}. Since the lifetime of this sensitizer on alumina, where electron injection is not observed, was around 0.26 s, the measured rate constants correspond to the electron injection rate constants. It is not clear how charge trapping and detrapping may affect the microwave absorption change measured. The calculated electron transfer rates showed an interesting correlation with the energy difference between the sensitizer excited-state oxidation potential and the energy of the semiconductor conduction band edge,

increasing with increasing driving force. Similar behavior had previously been observed for sensitized semiconductor powders [90].

Kamat has studied electron injection following excitation of $Ru(dcb)(bpy)_2^{2+}$ on SnO_2 with an applied external bias [83]. Biasing of nanocrystalline semiconductor films toward negative electrochemical potentials is known to directly reduce the material [23–35]. Positive biasing results in quenching of the photoluminescence and improved photocurrent responses in functional solar cells [83,88,91]. For negatively biased films, the low photocurrent may be due to: (a) enhanced charge recombination following electron injection; or (b) decreased electron injection yields [83]. The former would likely result in little change in the excited-state lifetime as the film is negatively biased. On the contrary, Kamat et al. observed longer excited-state lifetimes at negative bias leading the authors to conclude that the applied bias controls only the yield of electron injection [83]. The rate constant for electron injection was obtained from a comparison of the emission decay rates for $*Ru(dcb)(bpy)_2^{2+}$ on SiO_2 (no injection) and SnO_2 at an applied potential of 0.6 V versus Ag/AgCl, yielding 4.25×10^8 and 1.7×10^7 s^{-1} based on a biexponential fit [83]. Transient absorbance measurements were used to estimate the yield of the excited state, at 380 nm and oxidized complex at 397 nm. Based on the yield of oxidized dye, and assuming that the only fate of the excited state is electron injection, radiative and nonradiative decay, then the rate of electron injection was found to increase with increasingly positive applied potential from -0.6 to 0.4 V versus Ag/AgCl, reaching a plateau value of 4×10^8 s^{-1} [83]. The rate constant obtained from the transient absorbance yield measurements, the fast component of the time resolved photoluminescence experiments, and previously reported transient microwave conductivity measurements [89], are in agreement.

Heimer et al. studied the effect of reducing the through-bond electronic coupling between the sensitizer and the surface binding group by comparing the sensitizers $Ru(dmb)_2(bpy\text{-}COOH)^{2+}$, $Ru(dmb)_2(bpy\text{-}(CH_2)_3\text{–}COOH)^{2+}$ and $Ru(dmb)_2(bpy\text{-}acac)^{2+}$ on nanocrystalline thin films of TiO_2 immersed in 0.1 M $LiClO_4$ propylene carbonate [92]. Excitation was carried out at 532 nm with a 8 ns pulse width. The kinetics of electron injection were followed by monitoring the transient absorbance of the oxidized sensitizers at the ground state–excited state isosbestic point. In all cases, the rate of formation of the oxidized sensitizer could not be time resolved, implying $k_{inj} > 5 \times 10^7$ s^{-1}.

The rate of electron injection in thin ZnO semiconductor films, sensitized with surface bound $Ru(dcb)(bpy)_2^{2+}$, have been studied by Bedja et al. [91]. The reaction was studied by time resolved luminescence and microwave absorption exciting at 532 nm with a 6 ns pulse width. The emission decay was nonexponential and was fit to biexponential kinetics with lifetimes of 9.6 and 83 ns, respectively. Subtracting the excited-state lifetime on Al_2O_3 of 260 ns [86], yielded the reported electron injection rate constant, $k_{inj} = 10^8$ and 8×10^6 s^{-1} for the two components with the faster component comprising 78% of the decay [91]. Microwave adsorption experiments yielded a conductivity growth rate constant attributed to electron injection, $k_{inj} = 1.1 \times 10^8$ s^{-1}, in agreement with the fast component of the emission decay.

Photosensitization of SnO_2/CdS composite nanocrystalline thin films with $Ru(bpy)(bpy\text{-}C_6H_4\text{–}PO_3H_2)^{2+}$ has been reported by Nasr et al. [93]. The electron injection rate constant was obtained from a triexponential fit of the emission decay following excitation with a 6 ns, 532 nm laser pulse. The average excited-state lifetime on SiO_2, SnO_2 and SnO_2/CdS were found to be 90, 5.8 and 17.2 ns, respectively. It was suggested that an initial fast decay observed on SiO_2 might arise from an excited-state annihilation process. Electron injection rate constants on SnO_2 and SnO_2/CdS were calculated, $k_{inj} = 1.6 \times 10^8$ and 4.7×10^7 s^{-1}, respectively, assuming that the enhanced decay rates relative to that observed on SiO_2 are due solely to electron injection. The slower rate constant for injection into CdS was attributed to a ca. 100 mV endergonic driving force compared to a ca. 700 mV exergonic driving force for injection into SnO_2.

2.1.3. Ultra-fast transient absorbance measurements

The potential pit fall in the use of the photoluminescence decay for measuring the rate of electron injection is the assumption that electron injection is the only competitive reaction pathway responsible for excited state quenching. Microwave conductivity measurements suffer from uncertainty regarding the role of electron trapping and detrapping on the observed signal. To overcome these limitations, several groups have attempted to directly probe the rate of electron injection by transient absorption detection of the charge injection products, i.e. the oxidized dye or the injected electron.

The first such study on nanocrystalline thin films was conducted by Tachibana et al. who investigated *cis*-$Ru(dcb)_2(NCS)_2$ Fig. 4, on TiO_2 and ZrO_2 films immersed in 1:1 ethylene carbonate–propylene carbonate [94]. Comparison of the transient absorbance spectrum on the insulator ZrO_2 with that of the excited state in solution, i.e. a bleach of the ground state MLCT absorbance around 550 nm and an absorbance maximum at 720 nm attributed to an NCS^- to Ru^{3+} LMCT transition. In contrast, the transient spectrum observed on TiO_2 exhibits a more intense bleach at 550 nm and a shift of the long wavelength absorbance to 800 nm. This spectrum is consistent with that of the oxidized sensitizer generated transiently in solution by oxidative quenching of the excited state with methylviologen. The electron injection kinetics were probed at 750 nm following excitation at 605 nm with a 150–250 fs instrument response time. The absorbance growth at 750 nm exhibited biphasic kinetics with an approximately 50% growth occurring in < 150 fs and $\sim 50\%$ occurring in ~ 1.2 ps. It was suggested that the fast component may be electron injection from the initially populated singlet while the slow component is due to electron injection from the relaxed excited state.

Hannappel et al. followed up the work of Tachibana et al. [94], with the same photosensitizer, i.e. *cis*-$Ru(dcb)_2(NCS)_2$, adsorbed on TiO_2 [95]. However, the absorption spectrum of the oxidized metal complex, obtained by chemical oxidation in solution, was inconsistent with that reported by Tachibana et al. [94], displaying no absorbance beyond ca. 780 nm [95]. Exciting the sensitizer on TiO_2 in ultra-high vacuum, UHV, at 550 nm with a 75–150 fs laser pulse, Hannappel et al. observed a transient bleach, centered around 550 nm, assigned to the oxidized sensitizer. In

UHV, the transient absorption signal decayed to the baseline within ca. 5 s, whereas in ethanol a residual absorbance remained beyond this time interval. No evidence for excited state formation was found on the TiO_2 film. The authors reported that no absorption signal was observed to the red of about 750 nm [95], in disagreement with the earlier investigation [94]. However, a transient absorption signal was found to grow in upon progressing from the visible to 1100 nm, attributed to intraband absorption of the injected hot electrons [95]. Deconvolution of the absorbance growth at 1100 nm yielded a rise time < 25 fs, which was identical at room temperature and at 26 K.

Moser et al. noted that one-electron oxidized *cis*-$Ru(dcb)_2(NCS)_2$ is stable for only 0.1–1 s depending upon the protonation state of the carboxyl groups of the dcb ligand [96]. Fragmentation of *cis*-$Ru(dcb)_2(NCS)_2$ has been noted under steady-state conditions [97]. Chemical oxidation of the complex in ethanol resulted in degradation of the dye involving cleavage of the C=N bond. Chemical oxidation of the related complex $Ru(bpy)_2(NCS)_2$, reported to be less prone to oxidative decomposition than its carboxylated analog, with $Ce^{IV}(NH_4)_2(NO_3)_6$ in acetonitrile was found to give a spectrum similar, but blue shifted, to that reported by transient spectroscopy [94], with bands at 578 and 746 nm [96]. Subsequent oxidation was reported to result in the formation of another species with a spectrum similar to that reported by Hannappel et al. [95], with a maximum at 428 nm [94]. It was further noted that *cis*-$Ru(dcb)_2(NCS)_2$ was found to degrade on dry TiO_2, especially in the presence of light, and have suggested that the results of Hannappel et al. [95], that were obtained on dry TiO_2 under UHV conditions, may be due to measurements made on degraded samples [96]. In support of this point, transient spectra of purposely degraded samples displayed a transient spectrum [96], similar to that reported by Hannappel et al. [95].

Das and Kamat have carried out the one-electron oxidation of *cis*-$Ru(dcb)_2(NCS)_2$ in aqueous solution using the oxidizing radicals $N_3^{\bullet}$ and $Br_2^{\bullet -}$ generated by pulse radiolysis [98]. The product formed exhibited absorption bands at 320 and 740 nm, independent of oxidant, consistent with that reported by Tachibana et al. [94]. Extended γ-radiolysis of the sample, again using $N_3^{\bullet}$ and $Br_2^{\bullet -}$ as the oxidizing agents, results in the formation of a product exhibiting an absorbance maximum around 450 nm attributed to an oxidizing product. Hannappel et al. have observed the spectrum obtained by Tachibana et al. [94], when the *cis*-$Ru(dcb)_2(NCS)_2/TiO_2$ film is immersed in ethanol, at ambient pressure in an inert atmosphere and in air, at high excitation intensities [99]. It was noted that the organic dye perylene adsorbed on TiO_2 is kinetically well behaved only under UHV conditions and, therefore, this should also hold for *cis*-$Ru(dcb)_2(NCS)_2/TiO_2$ [99]. However, the evidence now suggests that the oxidized sensitizer studied by Hannappel et al. [95], is spectroscopically distinct from that studied by Tachibana et al. [95].

Heimer and Heilweil studied the related sensitizer $Ru(deeb)(bpy)_2^{2+}$ on TiO_2 immersed in dichloromethane using transient absorption in the mid-IR, 1600–1800 cm^{-1}, to probe the injected electron directly [100]. It was concluded that electron injection proceeds within 20 ps, limited by their instrument response time. The same authors furthered their investigations with studies of *cis*-$Ru(dcb)_2(NCS)_2$ and

cis-$Ru(dcb)_2(NCS)_2$ on nanostructured TiO_2 and ZrO_2 films using an excitation pulse width of ~ 250 fs at 590 nm [101]. Probing the injected electron at 1850 cm^{-1}, the absorbance growth occurred within the instrument response time of 350 fs, indicating $k_{inj} > 2.9 \times 10^{12}$ s^{-1} for both ruthenium(II) complexes. No absorbance growth at this wavelength was observed for the sensitizers on ZrO_2.

Ellingson et al. studied the *cis*-$Ru(dcb)_2(NCS)_2/TiO_2$ system in air by probing in the near- and mid-IR [102]. Probing the transient absorbance at 1.52 μm of *cis*-$Ru(dcb)_2(NCS)_2$ on the insulator ZrO_2 or in ethanol solution revealed an absorbance change not attributable to the charge separation products, i.e. oxidized sensitizer or the injected electron. This absorbance was attributed to either the excited state or a photodecomposition product. By probing in the mid-infrared the injected electron was probed directly to yield a charge injection time constant of 50 ± 25 fs, deconvoluted from the instrument response function at 4.63 and 4.9 μm. This time constant was consistent with that observed at 6.6 μm. However, there also existed a partial decay, with a time constant of ca. 50 fs, at this wavelength attributed to cooling or trapping of the injected electrons.

2.1.4. Excited state processes

Despite the controversies, the high time resolution transient absorption experiments provide strong support that electron injection is indeed a fast process, probably proceeding with rate constants exceeding 10^{12} s^{-1}. This is in stark contrast to studies carried out on longer time scales, often based on comparisons of the photoluminescent decay rates of the sensitizer on an insulator or semiconductor. A weakness of the photoluminescence experiments is that it is an indirect technique for measuring electron transfer reactions. The method is completely reliant on electron transfer being the sole contributor to enhanced decay rates on the semiconductor. However, the environments experienced by the sensitizer on different surfaces may, on their own, alter the lifetime of the excited state. A better approach would be to compare the excited state chemistry of the sensitizer on the surface of the same material, but under conditions where electron injection could be systematically turned on or off.

One strategy to control electron injection is to apply an external bias to the film, as discussed above. An alternative approach has been reported by Kelly et al. who have found that the efficiency of electron injection for nanocrystalline TiO_2 films of $Ru(deeb)(bpy)_2^{2+}$, abbreviated Ru^{2+}/TiO_2, immersed in acetonitrile, can be widely tuned by varying the electrolyte composition [103]. Fig. 7 shows the transient absorption difference spectra of Ru^{2+}/TiO_2 in neat acetonitrile after 532 nm, ~ 7 ns, excitation. The time resolved spectra shown are consistent with the MLCT excited state of the sensitizer with an absorption maximum at 380 nm, the bleach of the ground state MLCT transition at 475 nm, and a longer wavelength absorbance beyond 530 nm. The deviation of the ground/excited state isosbestic point at 403 nm has been attributed to the formation of the oxidized sensitizer, which is small in this case. By probing the absorbance change at the ground/excited state isosbestic point, the concentration of oxidized sensitizer can be directly measured, without interference from the excited state. This allows the excited state

and charge transfer reactions to be studied on the same semiconductor films simply by varying the electrolyte concentration.

The excited-state decay kinetics of Ru^{2+}/TiO_2 immersed in neat acetonitrile, probed by transient absorption spectroscopy at 380 and 475 nm, exhibited nonexponential kinetics [104]. By minimizing the excitation irradiance, near exponential kinetics were observed for the excited-state decay. However, at high excitation irradiance, second-order, equal concentration, kinetics were found to fit the experimental data well. These observations are consistent with competitive first- and second-order processes attributed to radiative and nonradiative excited state deactivation, Eq. (9), proceeding in parallel with excited-state annihilation, Eq. (10).

$$*Ru^{2+}/TiO_2 \rightarrow Ru^{2+}/TiO_2 + (h\nu \text{ or } \Delta) \quad (9)$$

$$2*Ru^{2+}/TiO_2 \rightarrow \text{Products} \quad (10)$$

A second-ordered contribution to the excited-state decay of $Ru(bpy)_3^{2+}$ adsorbed on surfactant or polymer modified nanocrystaline TiO_2 films has been reported by Rabani and co-workers [105]. The implied parallel first- and second-order kinetic model has successfully been used to fit many excited-state decays on nanocrystalline

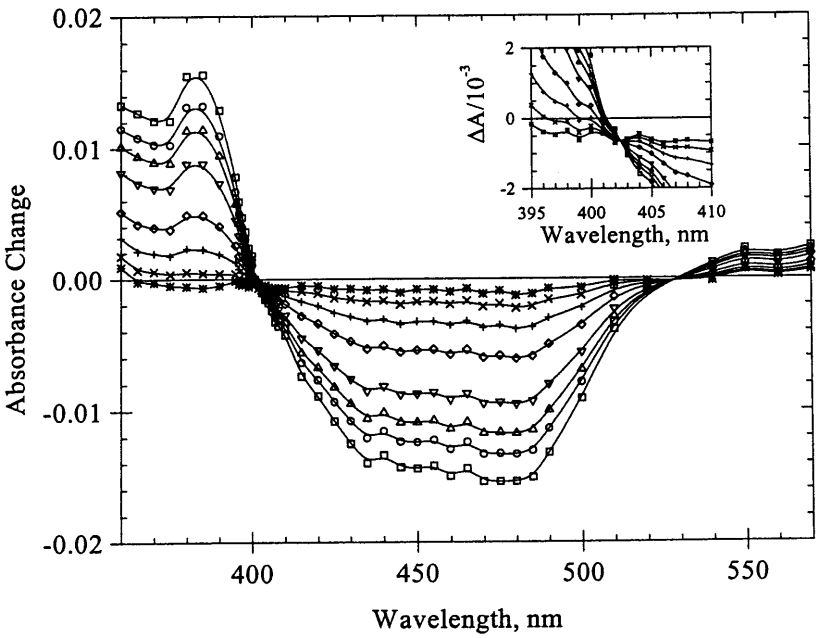

Fig. 7. Transient absorption spectrum following pulsed laser excitation (532 nm, ~7 ns) of $Ru(deeb)(bpy)_2^{2+}$ adsorbed on TiO_2 immersed in neat acetonitrile recorded at □: 0, ○: 50 ns, △: 100 ns, ▽: 200 ns, diamonds: 500 ns, +: 1 s and *: 4 s. The inset is an expansion of the 395–410 nm region of the spectrum. The spectrum is consistent with that of the excited state except for the deviation of the ground/excited state isosbestic point at 403 nm from zero. This deviation is attributed to the formation of the oxidized sensitizer as a result of electron injection into the TiO_2 semiconductor.

thin films in our laboratory. The possibility that the first- and second-order rate constants, obtained from fitting kinetic data to this model, represent an underlying distribution of rate constants cannot be ruled out [79]. However, such distributions were not required to fit the data with self consistent rate constants.

Kelly et al. have found that increasing the concentration of $LiClO_4$ in the acetonitrile electrolyte results in an enhancement of the electron injection yield, observed by probing the concentration of the oxidized sensitizer at the ground/excited state isosbestic point [103]. Remarkably, the injection quantum yield could be reversibly controlled by varying the Li^+ concentration. Other cations were found to exhibit a similar effect, but to a magnitude related to the charge/radius ratio of the cation. Cation control of the interfacial electron transfer reaction is a powerful tool for altering the reactivity of surface bound sensitizers. Biasing thin films of nanocrystalline TiO_2 in Li^+ or Na^+ electrolytes to negative electrochemical potentials is known to result in cation intercalation as a means of charge compensation [106–114]. In the presence of Li^+, the electrochemical potential for reduction of nanocrystalline TiO_2 is known to shift to more positive potentials in aprotic solvents such as acetonitrile, an effect attributed to surface association by the cation [115–117]. Therefore, the cation effect appears to be of thermodynamic origin, displaying an effect similar to that noted above for an applied external bias to the semiconductor film. In neat, dry acetonitrile, electron injection is minimized while the quantum yield for electron injection, $\phi(Ru^{3+})$, increases with increasing Li^+ concentration, Fig. 8. The trend of increasing electron injection quantum yield, approximately with the log[Li^+], is reproducible among different sensitized materials. However, the absolute yields exhibit a sample dependence, the origin of which is not yet well understood [103].

Increasing the concentration of Li^+ results in a parallel increase in both the yield of oxidized sensitizer and static photoluminesence quenching of $*Ru^{2+}/TiO_2$ (i.e. within the instrument response time of ca. 10 ns) [103]. These observations are consistent with ultra-fast electron injection, Eq. (2), which is expected to simultaneously deplete the excited state concentration and increase the oxidized ruthenium complex concentration within the 7 ns laser pulse. Concomitant with the static quenching was an increase in the rate of luminescence decay, i.e. dynamic quenching. As described above, dynamic quenching has been used as an indirect measure of the electron injection rate. Importantly however, the dynamic quenching kinetics with added Li^+ are not paralleled by an increase in concentration of oxidized sensitizer, as expected if the enhanced decay rate was attributable to electron injection. It has been proposed that the dynamic luminescent decay is due to oxidative quenching of the excited state by oxidized sensitizers (Eq. (11)) formed from electron injection (Eq. (2)) [103]

$$P^*/S + P^{\bullet+}(e^-) \rightarrow P^{\bullet+}/S + P/S(e^-) \tag{11}$$

Such a reaction would be favored by efficient migration of the hole [36,52], and excited state [104] on the surface. The net result of this surface quenching mechanism is loss of excited state, without a change in concentration of oxidized sensitizer. The quenching rate, Eq. (11), is proportional to the concentration of oxidized sensitizer, $P^{\bullet+}/S(e^-)$. Consequently, we believe that the key assumption

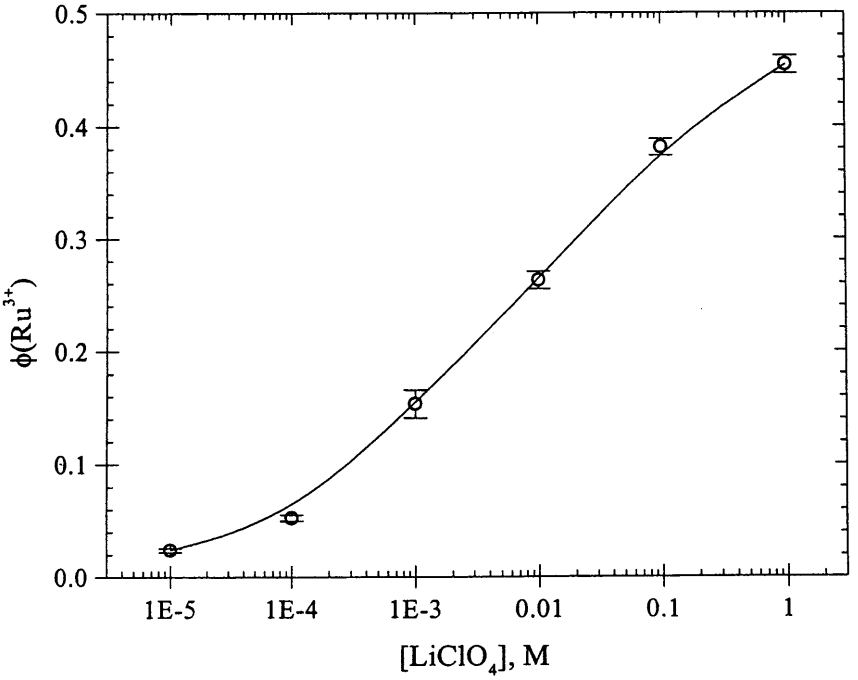

Fig. 8. Quantum yields for the formation of oxidized sensitizer, $\phi(Ru)^{3+}$ as a function of $[LiClO_4]$ in the $Ru(deeb)(bpy)_2^{2+}/TiO_2$ system in acetonitrile following a ca. 7 ns,532 nm laser excitation pulse at 25°C. The measurements were made at 403 nm assuming the extinction coefficient difference between the ground and oxidized state is $-6200\ M^{-1}\ cm^{-1}$. The excitation intensity was $3.7 \pm 0.2 \times 10^{-6}$ Einsteins/L determined by comparative actinometry with $Ru(bpy)_3^{2+}$ in acetonitrile [21]. The absolute values of the quantum yields are sample dependent.

regarding the use of excited state lifetime measurements as an indirect probe of the electron injection injection rate constant is invalid for these materials, under these conditions. An interesting kinetic dilemma arises due to the observation of long lived excited states on semiconductor surfaces where electron injection is known to occur [103]. If electron injection proceeds in competition with other excited-state decay pathways, and if the rate of electron injection is orders of magnitude faster than the other processes (as appears to be the case), then the excited state should decay with a rate constant identical to that for electron injection. The observation of both fast electron injection and long-lived excited states implies two distinct populations of excited states, i.e. those that are capable, and those that are incapable, of electron injection. Interestingly, in measurements made with sufficiently high time resolution, electron injection proceeds on time scales that are competitive with thermal equilibration to the lowest lying excited state of the sensitizer [118]. Such observations are consistent with the idea that electron injection proceeds only from upper, i.e. non-thermally equilibrated or, excited states, in competition with thermal relaxation to the thermally equilibrated excited, or thexi, state of the sensitizer, Fig.

9 [119]. The thermally equilibrated MLCT excited state of the sensitizer subsequently decays by processes not involving electron injection.

3. Conclusions

A clear picture of the photochemistry and photophysics of metallo-bipyridine complexes on the surface of semiconductors is rapidly evolving. Although gaps exist and there are undoubtedly differences associated with sensitizer, medium, and semiconductor variation, a rough draft of the mechanistic details can now be sketched out. Electronic excitation of the sensitizer results in electron injection with a rate constant exceeding about 1×10^{12} s^{-1}, possibly on time scales competitive with thermal equilibration to the lowest lying excited state of the sensitizer. The lowest lying excited state of $Ru(dcb)(bpy)_2^{2+}$ appears to be incapable of electron injection into TiO_2 (anatase). Variation of the electron injection rate constant by electrolyte composition or applying an external bias to the film can alter the relative quantum yields for electron injection and population of the long-lived MLCT excited state. The ensemble of thermally equilibrated MLCT excited states decay by a composite reaction mechanism. This mechanism has been proposed to include first-order radiative and nonradiative decay pathways in parallel with a second-order process attributed to excited state annihilation and a bimolecular process associated with oxidative quenching by surface bound, oxidized sensitizers. In the absence of electron injection, i.e. on an insulator surface, the latter process does not occur, resulting in longer lived excited states. The second-order component of the excited-state decay is due to excited state-excited state interactions and is the result

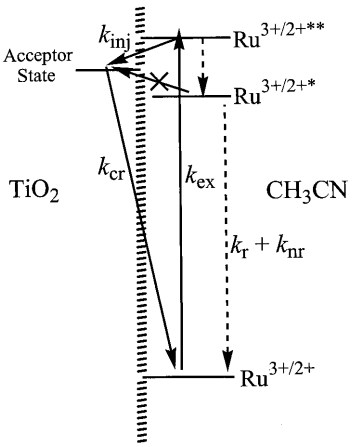

Fig. 9. Model to account for two populations of $Ru(deeb)(bpy)_2^{2+}/TiO_2$ excited states in acetonitrile electrolyte. The species $Ru^{2+}**$ is a non-thermally equilibrated, or hot, excited state of the sensitizer that decays by competitive electron injection and internal conversion/intersystem crossing, and $Ru^{2+}*$ represents the thermally equilibrated MLCT excited state that, in this model, is energetically incapable of electron injection.

of the high density of sensitizers on the semiconductor surface. The establishment of a mechanism provides a starting point from which surface mediated excited state chemistry can be predicted and manipulated.

Acknowledgements

The National Science Foundation (CHE-9322559, CHE-9402935), and the Division of Chemical Sciences, Office of Basic Energy Sciences, Office of Energy Research, US Department of Energy are gratefully acknowledged for research support.

References

[1] H.D. Gafney, A.W. Adamson, J. Am. Chem. Soc. 94 (1972) 8238.
[2] A.W. Adamson, Physical Chemistry of Surfaces, Wiley, New York, 1990.
[3] T. Gerfin, M. Grätzel, L. Walder, Prog. Inorg. Chem. 44 (1997) 345.
[4] K. Kalyanasundaram, M. Grätzel, Coord. Chem. Rev. 77 (1998) 347.
[5] K.L. Hardee, A.J. Bard, J. Electrochem. Soc. 124 (1977) 215.
[6] M.S. Wrighton, Acc. Chem. Res. 12 (1979) 303.
[7] H. Meier, Photochem. Photobiol. 16 (1972) 219.
[8] K. Hauffe, H.J. Danzmann, H. Pusch, J. Range, H. Volz, J. Electrochem. Soc. 117 (1970) 993.
[9] H. Tributsch, M. Calvin, Photochem. Photobiol. 14 (1971) 95.
[10] H. Gerischer, Photochem. Photobiol. 16 (1972) 243.
[11] R. Memming, Photochem. Photobiol. 16 (1972) 325.
[12] M. Gleria, R. Memming, Z. Phys. Chem. 98 (1975) 303.
[13] W.D.K. Clark, N. Sutin, J. Am. Chem. Soc. 99 (1977) 4676.
[14] The light harvesting efficiency, LHE, is the fraction of incident radiant power absorbed and is equivalent to absorbance: J.W. Verhoeven, Pure Appl. Chem. 68 (1996) 2223.
[15] A.J. Nozik, Ann. Rev. Phys. Chem. 29 (1978) 189.
[16] J. Desilvestro, M. Grätzel, L. Kavan, J. Moser, J. Augustynski, J. Am. Chem. Soc. 107 (1985) 2988.
[17] N. Vlachopoulos, P. Liska, J. Augustynski, M. Grätzel, J. Am. Chem. Soc. 110 (1988) 1216.
[18] P. Liska, N. Vlachopoulos, M.K. Nazeeruddin, P. Comte, M. Grätzel, J. Am. Chem. Soc. 110 (1988) 3686.
[19] M.K. Nazeeruddin, P. Liska, J. Moser, N. Vlachopoulos, M. Grätzel, Helv. Chim. Acta 73 (1990) 1788.
[20] B.O Regan, M. Grätzel, Nature 353 (1991) 737.
[21] C.A. Kelly, G.J. Meyer, unpublished results.
[22] A. Hagfeldt, M. Grätzel, Chem. Rev. 95 (1995) 49.
[23] B.O Regan, M. Grätzel, D. Fitzmaurice, Chem. Phys. Lett. 183 (1991) 89.
[24] B.O Regan, M. Grätzel, D. Fitzmaurice, J. Phys. Chem. 95 (1991) 10525.
[25] G. Redmond, D. Fitzmaurice, J. Phys. Chem. 97 (1993) 1426.
[26] G. Redmond, D. Fitzmaurice, M. Grätzel, J. Phys. Chem. 97 (1993) 6951.
[27] I. Bedja, S. Hotchandani, P.V. Kamat, J. Phys. Chem. 97 (1993) 11064.
[28] A. Hagfeldt, N. Vlachopoulos, M. Grätzel, J. Electrochem. Soc. 141 (1994) L82.
[29] S. Hotchandani, I. Bedja, R.W. Fessenden, P.V. Kamat, Langmuir 10 (1994) 17.
[30] F. Cao, G. Oskam, P.C. Searson, J.M. Stipkala, T.A. Heimer, F. Farzad, G.J. Meyer, J. Phys. Chem. 99 (1995) 11974.
[31] S. Doherty, D. Fitzmaurice, J. Phys. Chem. 100 (1996) 10732.

[32] G.K. Boschloo, A. Goossens, J. Schoonman, J. Electroanal. Chem. 428 (1997) 25.
[33] G. Boschloo, D. Fitzmaurice, J. Phys. Chem. B 103 (1999) 2228.
[34] B.O Regan, J. Moser, M. Anderson, M. Grätzel, J. Phys. Chem. 94 (1990) 8720.
[35] P.V. Kamat, I. Bedja, S. Hotchandani, L.K. Patterson, J. Phys. Chem. 98 (1994) 4133.
[36] P. Bonhôte, E. Gogniat, S. Tingry, C. Barb, N. Vlachopoulos, F. Lenzmann, P. Comte, M. Grätzel, J. Phys. Chem. 102 (1998) 1498.
[37] G.J. Meyer, P.C. Searson, Interface (1993) 23.
[38] T.A. Heimer, G.J. Meyer, Proc. Electrochem. Soc. 95–98 (1994) 167.
[39] G.J. Meyer, J. Chem. Educ. 74 (1997) 652.
[40] S.G. Yan, L.A. Lyon, B.I. Lemon, J.S. Preiskorn, J.T. Hupp, J. Chem. Educ. 74 (1997) 657.
[41] R.F. Howe, M. Grätzel, J. Phys. Chem. 89 (1985) 4495.
[42] S.A. Haque, Y. Tachibana, D.R. Klug, J.R. Durrant, J. Phys. Chem. B 102 (1998) 1745.
[43] F. Cao, G. Oskam, G.J. Meyer, P.C. Searson, J. Phys. Chem. 96 (1992) 5983.
[44] A. Solbrand, H. Lindstr m, H. Rensmo, A. Hagfeldt, S.-E. Lindquist, J. Phys. Chem. 101 (1997) 2514.
[45] P.E. De Jongh, D. Vanmaekelbergh, J. Phys. Chem. B 101 (1997) 2716.
[46] A. Zaban, A. Meier, B.A. Gregg, J. Phys. Chem. B 101 (1997) 7985.
[47] A. Shiga, A. Tsujiko, T. Ide, S. Yae, Y. Nakato, J. Phys. Chem. B 102 (1998) 6049.
[48] A. Wahl, J. Augustynski, J. Phys. Chem. B 102 (1998) 7820.
[49] G. Franco, J. Gehring, L.M. Peter, E.A. Ponomarev, I. Uhlendorf, J. Phys. Chem. B 103 (1999) 692.
[50] D. Vanmaekelbergh, P.E. de Jongh, J. Phys. Chem. B 103 (1999) 747.
[51] G. Schlichthörl, N.G. Park, A.J. Frank, J. Phys. Chem. B 103 (1999) 782.
[52] S.A. Trammell, T.J. Meyer, J. Phys. Chem. B 103 (1999) 104.
[53] A. Henglein, Chem. Rev. 89 (1989) 1861.
[54] E. Matijevic, Langmuir 2 (1986) 12.
[55] J.J. Ramsden, Proc. R. Soc. Lond. Ser. A. 410 (1987) 89.
[56] H. Weller, Adv. Mater. 5 (1993) 88.
[57] T.A. Heimer, G.J. Meyer, J. Lumin. 70 (1996) 468.
[58] P.V. Kamat, Chem. Rev. 93 (1993) 267.
[59] P.V. Kamat, Prog. Inorg. Chem. 44 (1997) 273.
[60] M.A. Fox, F.J. Nobs, T.A. Voynick, J. Am. Chem. Soc. 102 (1980) 4029.
[61] M.A. Fox, F.J. Nobs, T.A. Voynick, J. Am. Chem. Soc. 102 (1980) 4036.
[62] R. Dabestani, A.J. Bard, A. Campion, M.A. Fox, T.E. Mallouk, S.E. Webber, J.M. White, J. Phys. Chem. 92 (1988) 1872.
[63] W.E. Ford, M.A.J. Rodgers, J. Phys. Chem. 98 (1994) 3822.
[64] W.E. Ford, M.A.J. Rodgers, J. Phys. Chem. 99 (1995) 5139.
[65] W.E. Ford, J.M. Wessels, M.A.J. Rodgers, Langmuir 12 (1996) 3449.
[66] J.M. Wessels, C.S. Foote, W.E. Ford, M.A.J. Rodgers, Photochem. Photobiol. 65 (1997) 96.
[67] W.E. Ford, M.A.J. Rodgers, J. Phys. Chem. B 101 (1997) 930.
[68] W.E. Ford, J.M. Wessels, M.A.J. Rodgers, J. Phys. Chem. B 101 (1997) 7435.
[69] J. Moser, M. Grätzel, D.K. Sharma, N. Serpone, Helv. Chim. Acta 68 (1985) 1686.
[70] J.E. Moser, M. Grätzel, Chem. Phys. 176 (1993) 493.
[71] P.V. Kamat, J. Phys. Chem. 93 (1989) 859.
[72] P.V. Kamat, Langmuir 6 (1990) 512.
[73] P.V. Kamat, B. Patrick, Electrochemistry, in: R.A. Mackay, J. Texter (Eds.), Colloids and Dispersions, VCH, New York, 1992, p. 447.
[74] B. Patrick, P.V. Kamat, J. Phys. Chem. 96 (1992) 1423.
[75] N. Sutin, J. Photochem. 10 (1979) 19–40.
[76] C.A. Bignozzi, J.R. Schoonover, F. Scandola, Prog. Inorg. Chem. 44 (1997) 1.
[77] I. Ortmans, C. Moucheron, A. Kirsch-De Mesmaeker, Coord. Chem. Rev. 168 (1998) 233.
[78] D.W. Thompson, C.A. Kelly, F. Farzad, G.J. Meyer, Langmuir 15 (1999) 650.
[79] H.P. Lu, X.S. Xie, J. Phys. Chem. B 101 (1997) 2753.
[80] E.R. Carraway, J.N. Demas, B.A. DeGraff, Anal. Chem. 63 (1991) 332.

[81] T.A. Heimer, G.J. Meyer, J. Lumin. 70 (1996) 468.
[82] R. Eichberger, F. Willig, Chem. Phys. 141 (1990) 159.
[83] P.V. Kamat, I. Bedja, S. Hotchandani, L.K. Patterson, J. Phys. Chem. 100 (1996) 4900.
[84] K. Vinodgopal, X. Hua, R.L. Dahlgren, A.G. Lappin, L.K. Patterson, P.V. Kamat, J. Phys. Chem. 99 (1995) 10883.
[85] F. Willig, R. Keitzmann, K. Schwarzburg, Proceedings of the International Symposium on Optical Materials Technology for Energy Efficiency and Solar energy, SPIE, 1992.
[86] I. Bedja, S. Hotchandani, P.V. Kamat, J. Phys. Chem. 98 (1994) 4133.
[87] T.A. Heimer, G.J. Meyer, Proc. Electrochem. Soc. 95-98 (1994) 167.
[88] R. Argazzi, C.A. Bignozzi, T.A. Heimer, F.N. Castellano, G.J. Meyer, Inorg. Chem. 33 (1994) 5741.
[89] R.W. Fessenden, P.V. Kamat, J. Phys. Chem. 99 (1995) 12902.
[90] T. Sakata, K. Hashimoto, M. Hiramoto, J. Phys. Chem. 94 (1990) 3040.
[91] I. Bedja, P.V. Kamat, X. Hua, A.G. Lappin, S. Hotchandani, Langmuir 13 (1997) 2398.
[92] T.A. Heimer, S.T.D Arcangelis, F. Farzad, J.M. Stipkala, G.J. Meyer, Inorg. Chem. 35 (1996) 5319.
[93] C. Nasr, S. Hotchandani, W.Y. Kim, R.H. Schmehl, P.V. Kamat, J. Phys. Chem. B 38 (1997) 7480.
[94] Y. Tachibana, J.E. Moser, M. Grätzel, D.R. Klug, J.R. Durrant, J. Phys. Chem. 100 (1996) 20056.
[95] T. Hannappel, B. Burfeindt, W. Storck, F. Willig, J. Phys. Chem. B 101 (1997) 6799.
[96] J.E. Moser, D. Noukakis, U. Bach, Y. Tachibana, D.R. Klug, J.R. Durrant, R. Humphry-Baker, M. Grätzel, J. Phys. Chem. B 102 (1998) 3649.
[97] R. Grünwald, H. Tributsch, J. Phys. Chem. B 101 (1997) 2564.
[98] S. Das, P.V. Kamat, J. Phys. Chem. A 102 (1998) 8954.
[99] T. Hannappel, C. Zimmermann, B. Meissner, B. Burfeindt, W. Storck, F. Willig, J. Phys. Chem. B 102 (1998) 3651.
[100] T.A. Heimer, E.J. Heilweil, J. Phys. Chem. B 101 (1997) 10990.
[101] T.A. Heimer, E.J. Heilweil, in: T. Elsaesser, J.G. Fujimoto, D.A. Wiersma, W. Zinth (Eds.), Ultrafast Phenomena, vol. XI, Springer, Berlin, 1998, p. 505.
[102] C.A. Kelly, F. Farzad, D.W. Thompson, J.M. Stipkala, G.J. Meyer, Langmuir 15 (1999) 7047.
[103] R.J. Ellingson, J.B. Asbury, S. Ferrere, H.N. Ghosh, J.R. Sprague, T. Lian, A.J. Nozik, J. Phys. Chem. B 102 (1998) 6455.
[104] J. Rabani, K. Ushida, K. Yamashita, J. Stark, S. Gershuni, A. Kira, J. Phys. Chem. B 101 (1997) 3136.
[105] A. Hagfeldt, N. Vlachopoulos, S. Gilbert, M. Grätzel, Proc. SPIE 2255 (1994) 297.
[106] S. Huang, L. Kavan, A. Kay, M. Grätzel, Act. Pass. Elec. Comp. 18 (1995) 23.
[107] S. Huang, L. Kavan, I. Exnar, M. Grätzel, J. Electrochem. Soc. 142 (1995) 142.
[108] L.A. Lyon, J.T. Hupp, J. Phys. Chem. 99 (1995) 15718.
[109] B. Zachau-Christiansen, K. West, T. Jacobsen, S. Atlung, Solid State Ionics 28 (1988) 1176.
[110] A. Stashans, S. Lunell, R. Bergstr m, A. Hagfeldt, S.-E. Lindquist, Phys. Rev. B 53 (1996) 159.
[111] H. Lindstr m, S.S dergren, A. Solbrand, H. Rensmo, J. Hjelm, A. Hagfeldt, S.-E. Lindquist, J. Phys. Chem. B 101 (1997) 7710.
[112] S. Lunell, A. Stashans, L. Ojam e, H. Lindstr m, A. Hagfeldt, J. Am. Chem. Soc. 119 (1997) 7374.
[113] L. Benco, J.-L. Barras, C.A. Daul, E. Deiss, Inorg. Chem. 38 (1998) 20.
[114] J. Augustynski, Struct. Bonding 69 (1988) 1.
[115] B. Enright, G. Redmond, D. Fitzmaurice, J. Phys. Chem. 98 (1994) 6195.
[116] H. Lindstr m, S.S dergren, A. Solbrand, H. Rensmo, J. Hjelm, A. Hagfeldt, S.-E. Lindquist, J. Phys. Chem. B 101 (1997) 7717.
[117] N.H. Damrauer, G. Cerullo, A. Yeh, T.R. Boussie, C.V. Shank, J.K. McCusker, Science 275 (1997) 54.
[118] A.W. Adamson, J. Chem. Educ. 60 (1983) 797.
[119] C.A. Kelly, F. Farzad, D.W. Thompson, G.J. Meyer, Langmuir 15 (1999) 731.